

CORRESPONDENCE

Comments on “Global and Regional Entropy Production by Radiation Estimated from Satellite Observations”

GOODWIN GIBBINS^a AND JOANNA D. HAIGH^{a,b}

^a *Imperial College London, London, United Kingdom*

^b *Grantham Institute–Climate Change and the Environment, Imperial College London, London, United Kingdom*

(Manuscript received 28 August 2020, in final form 21 January 2021)

ABSTRACT: A recent paper by Kato and Rose reports a negative correlation between the annual mean entropy production rate of the climate and the absorption of solar radiation in the CERES SYN1deg dataset, using the simplifying assumption that the system is steady in time. It is shown here, however, that when the nonsteady interannual storage of entropy is accounted for, the dataset instead implies a *positive* correlation; that is, global entropy production rates *increase* with solar absorption. Furthermore, this increase is consistent with the response demonstrated by an energy balance model and a radiative–convective model. To motivate this updated analysis, a detailed discussion of the conceptual relationship between entropy production, entropy storage, and entropy flows is provided. The storage-corrected estimate for the mean global rate of entropy production in the CERES dataset from all irreversible transfer processes is $81.9 \text{ mW m}^{-2} \text{ K}^{-1}$ and from only nonradiative processes is $55.2 \text{ mW m}^{-2} \text{ K}^{-1}$ (observations from March 2000 to February 2018).

KEYWORDS: Albedo; Budgets; Climatology; Entropy; Satellite observations; Interannual variability

1. Introduction

In Kato and Rose (2020, hereinafter KR2020), a useful new dataset is introduced and explored that leverages the satellite-derived CERES data products to estimate Earth’s entropy production rates monthly since March 2000. The global entropy production rate is an underexplored variable that many have hypothesized could furnish a new predictive theory of the climate (Paltridge 1975; Ozawa 2003; Martyushev and Seleznev 2006). The existence of such a thorough observational dataset is therefore a major step for the field but requires parallel development of the conceptual treatment of entropy production in realistic, nonidealized systems, in particular ones that are not steady in time and that have imbalanced top-of-atmosphere energy fluxes, as is the case in the climate today. In these unsteady cases, not only can entropy flow into and out of the system and be produced within the system, it can also be stored [as discussed in Bannon and Lee (2017)].

Entropy storage is addressed in passing in KR2020 but is not sufficiently established as a process distinct from entropy production and flow. Unfortunately, one of their headline conclusions—that the entropy production rate decreases when absorption of shortwave radiation increases—is contingent on the (incorrect) assumption that the observed climate system is in steady state and that therefore the storage of entropy can be neglected. In our reanalysis, we show that their result is *reversed* if the interannual storage of entropy in the


system is taken into account: the dataset that they introduce in fact suggests that the rate of global entropy production *increases* with increasing solar absorptivity, rather than decreasing as they conclude. Furthermore, this updated analysis brings the observational results in line with the entropy production rate behavior suggested by two simple steady-state climate models.

Ambiguity between the concepts of entropy flow, production, and storage is not unique to KR2020; indeed, more broadly in this field, our conceptual frameworks for describing the climate’s entropy production rates have not yet been fully codified and even the most fundamental definitions continue to be in active development (e.g., Goody 2000; Bannon 2015; Gibbins and Haigh 2020). This presents an unavoidable challenge for any study of entropy production results, especially one tasked with introducing a novel analysis of a new dataset, as in the paper under discussion.

Accordingly, we begin this comment by offering a careful framework for the concepts of entropy fluxes, productions, and storages, with the divergences between our understanding and the description offered in KR2020 highlighted (section 2). This then leads to the updated analysis of the KR2020 dataset, which we provide in section 3, where the rate of entropy storage in the climate system implied by the CERES SYN1deg dataset is explicitly estimated and used to correct the calculation of the global entropy production rates.

2. Entropy fluxes, production, and storage

To make sense of, analyze, and communicate observations of a physical system, definitions that make careful distinctions between the types of physical processes happening are crucial. Here, we offer an exposition from first principles that highlights three distinct types of entropy-changing processes

 Denotes content that is immediately available upon publication as open access.

Corresponding author: Goodwin Gibbins, r.gibbins15@imperial.ac.uk

(section 2a): flows, production, and storage. This is a summary and development of ideas discussed elsewhere in the literature, notably in Bannon (2015) and Bannon and Lee (2017). In section 2b, the areas of difference between this account and the one given in KR2020 are highlighted. In section 2c, the types of global entropy production rates that are measured are discussed.

a. *Entropy flow, production, and storage—From first principles*

Entropy production is an extensive process—two Earths would produce twice as much entropy as one Earth—and so whenever a production rate is specified, a system and a boundary between it and the surroundings are necessarily implied. Note that this may not be a simple physical dividing line, but might be, for example, the division between matter and radiation. A boundary implies that there can be cross-boundary flows (e.g., of energy in the case of the climate system). Energy delivered as heat at a rate F (W m^{-2}) to an object at temperature T increases the entropy of that object at a rate F/T , and similarly for energy extracted as cooling, which reduces the entropy by the same amount.¹ Thus, if energy crosses a boundary, entropy can be said to flow with it into and out of the system. We denote these entropy flows by J .

By contrast, we would argue that the concept of a *production* of entropy, denoted here Σ , should refer to an occasion where the total entropy of the universe increases. Entropy is special in that it can, and does, increase, since it can be created, unlike conserved quantities. A conserved quantity can increase locally by flowing, but this is a movement and not a production. Entropy production occurs with an irreversible downgradient heat transfer, or conversion of energy from one form to another (e.g., radiation, phase changes, and kinetic energy conversions) and is always positive. It will generally have the form of a heat transfer rate F multiplied by a difference in *two* inverse temperatures, $(1/T_C) - (1/T_H)$, where T_C is the colder of the temperatures. If there were no cross-boundary flows of entropy to reset the system, internal entropy production would ultimately result in the system achieving equilibrium in a maximum entropy state.

Entropy production can occur within a system, outside of a system, or during the process by which energy crosses into a system. Some flows of energy and entropy into a system involve an entropy production, such as the irreversible thermalization of solar radiation upon absorption by matter, but some do not, such as the crossing of photons from the sun through the top-of-the-atmosphere control volume [e.g., CV1 in Bannon (2015)]. The total entropy production rate of a system is the sum of the entropy productions that occurs *within* the system. Production occurring outside of the system of interest—for example, the irreversibility within the sun—is clearly not to be included in a climatological entropy production rate. Likewise, entropy production that occurs at the boundary of a system belongs to the surroundings and not to system; from the system's point of view, only the entropic impact of energy upon deposit within the system is knowable, and the same energy

delivery by a different mechanism involving a different amount of irreversibility would be indistinguishable (Gibbins and Haigh 2020). Careful description of the system's boundaries is essential for distinguishing the production rate.

Storage of entropy within (or extraction from) the system occurs when the total entropy content of the system changes, either due to production or due to imbalances in the entropy flows. Entropy storage is often associated with a storage of energy or can be due to a change in the distribution of energy and temperatures within the system and will likely occur only in any system that is not steady in time. Unlike production, storage can be temporary and can be reversed: positive storage of entropy in summer months is nearly balanced by extraction in winter months in the climate system. The rate of storage is a time derivative of the entropy of a system S and can be calculated like a flow of entropy into an internal reservoir at rate $dS_{\text{system}}/dt = F/T_{\text{stor}}$, where T_{stor} is the appropriately averaged storage temperature.

Entropy storage, flows, and productions must balance, and the relationship can be expressed (Bannon 2015; Bannon and Lee 2017) as

$$dS_{\text{system}}/dt = J_{\text{in}} - J_{\text{out}} + \Sigma, \quad (1)$$

where J_{in} and J_{out} are the entropy fluxes into and out of the system, as measured from the system's perspective; Σ is the entropy production rate within the system, measuring the total rate of irreversibility; and the storage of entropy within the system is the rate of change of the entropy content of the system: dS_{system}/dt . In a steady system, Eq. (1) simplifies considerably because $dS_{\text{system}}/dt = 0$ and so $\Sigma = J_{\text{out}} - J_{\text{in}}$.

b. *Divergences from Kato and Rose (2020)*

Our analysis is broadly consistent with Kato and Rose (2020), but the terminology introduced in their section 2 leads to some confusing and problematic consequences.

For example, KR2020's Eq. (5) (reproduced below for convenience),

$$J_{\text{TOA}}^{\text{net}} = J_{\text{ref}} - J_{\text{atm}} - (1 - \epsilon)J_{\text{sfc}} + (1 - \alpha)J_{\text{sun}},$$

is stated to be entropy export to space by radiation, which appears to be defined positive inward when examining the last three entropy flux terms on the right-hand side. However, J_{ref} is the (positive definite) entropy *produced* by the scattering of shortwave radiation, which results in a net export of entropy from the system and so should appear with a negative sign. In terms of fluxes only, the net top-of-atmosphere entropy export can be written [like Eq. (5.4) in Bannon (2015), but defined as positive inward]:

$$J_{\text{TOA}}^{\text{net}} = J_{\text{in}}^{\text{TOA}} - J_{\text{out}}^{\text{TOA}} = J_{\text{sun}} - J_{\text{scat}} - J_{\text{atm}} - (1 - \epsilon)J_{\text{sfc}}, \quad (2)$$

where J_{scat} is the entropy content of the scattered solar radiation and $(\alpha J_{\text{sun}} - J_{\text{scat}})$ can be recognized as KR2020's $-J_{\text{ref}}$ in terms of the albedo α .

There are more examples of awkward terminology in the subsequent six equations. KR2020's Eqs. (6) and (7) are labeled as productions but measure the net entropy flux into the

¹ Interestingly, this can be taken as a *definition* of temperature: a measure of the amount that the entropy of a system changes when heat is delivered to, or taken from, it.

surface and atmosphere, F_{net}/T , which is actually the rate of change of the stored entropy and is zero at steady state because of the energy balance requirements. There is also a case of a negative production—in KR2020's Eq. (10) for the production due to the emitted longwave irradiance—that can be confirmed by noting that the sum of the productions in KR2020's Eqs. (9)–(11) is zero in steady state. There are also values that are labeled as productions but are of the form $F/T = J$ and not a difference of J s, such as Eq. (9), which would need an additional term $[-(4/3)(1 - \alpha)F_{\text{sun}}/T_{\text{sun}}]$ to be the rate of production due to absorbed shortwave irradiance, as it is labeled, rather than the flux of entropy into the material system by absorption, as the current equation suggests.

In KR2020's Eqs. (14)–(18), an analysis is offered that is consistent with our Eq. (1). However, in discussing its application away from steady state, the authors suggest following an option outlined in Bannon and Lee (2017) to “subsume [the entropy storage] into entropy production within the system.” That text actually appears to suggest that one option is to combine the storage and production into a *new* “net production” term. Although the production and storage have the same units and so can be added into a combined variable, this variable would no longer be a straightforward entropy production rate of the system. Separating out storage to extract the entropy production rate in a nonsteady system is the focus of the next section.

c. Which entropy production rate?

Before proceeding, we note that these distinctions between productions, flows, and storage are wholly separate from the question of what the most relevant global entropy production rate is to describe the climate system—and in particular to what extent radiative processes should be included. This is not yet a settled question (Essex 1984; Goody and Abdou 1996; Goody 2000; Bannon 2015; Gibbins and Haigh 2020). The Kato and Rose (2020) paper is significant in that it makes a clear distinction between the entropy production rate due to purely nonradiative processes (the “material” entropy production rate) and the entropy production rate due to all internal irreversible processes, including that due to internal radiative transfer. In Gibbins and Haigh (2020), the latter is labeled the “transfer” entropy production rate. KR2020 is one of the first papers to focus on this transfer entropy production rate and to develop datasets for estimating it. The flows of entropy into and out of the material and transfer climate systems differ, as do the total production rates, but because the majority of the storage is shared in thermal reservoirs within the climate system, the storage discussion in the following section applies equally to both system perspectives.

3. Entropy production increases with increasing solar absorption

In Kato and Rose (2020), the *negative* correlation found is between the annual mean absorptivity of shortwave radiation and the net entropy export. This net export is the difference between entropy delivered to the system by absorption of shortwave radiation and that exported by emission of longwave radiation, $J_{\text{out}} - J_{\text{in}}$ in our notation (their Fig. 8, third panel).

The result is described as indicating a negative correlation between shortwave absorption and the “entropy production by irreversible processes.” However, rearranging Eq. (1), we can see that, in a system that is not steady and so has a nonzero rate of entropy storage, the difference in fluxes on which KR2020 focuses is actually a measure of the difference between the entropy production rate and the entropy storage rate:

$$J_{\text{out}} - J_{\text{in}} = \Sigma - \frac{dS_{\text{system}}}{dt}, \quad (3)$$

which is a very different variable. That storage might have an impact on their results is acknowledged in passing in KR2020, where it is noted that energy storage by the ocean results in a damping of the longwave emission anomaly and that “these smoothing or damping processes seem to be responsible for [the observed] negative [correlation]” (KR2020, 2994–2995). However, it is not subsequently accounted for. In this section we estimate the rate of entropy storage in the ocean in order to isolate the global entropy production rate. Doing so adjusts upward the estimate of the entropy production rates and uncovers a *positive* correlation between the productions Σ and shortwave absorptivity.

That more energy delivered to the system should increase the rate of irreversibility within the system is an intuitive result and one that is corroborated by the simple energy balance model described in Bannon (2015) and used in KR2020, and also by the analytic radiative–convective model used in Gibbins and Haigh (2020). This is explored in section 3d.

The same dataset as used by KR2020 has been obtained for this analysis; the CERES Edition 4.1 SYN1deg-Month data product introduced in Wielicki et al. (1996) and the entropy components added by KR2020 are available to download freely from CERES (<https://ceres.larc.nasa.gov/data/>). We can confirm that their results as described are independently reproducible from their datasets.² To match their analysis, we use the range from March 2000 to February 2018 and take March–February annual means, accounting for unequal month lengths and adjusting area averages for the oblate spheroid Earth on which the CERES data are described.

In KR2020, the CERES Energy Balance and Filled (CERES EBAF-TOA Ed4.1) product (Loeb et al. 2018) is used for estimating energy fluxes because it is, given that it has been adjusted to match observations of the average ocean heat storage rate, more accurate. However, because entropy flux J is closely related to energy flux F via $J = F/T$, mixing estimates for entropy and energy from different sources can introduce additional errors. All values quoted below use the SYN1deg data product, except where otherwise specified. EBAF energy flux values are used to calculate the annual SW absorption anomaly, for consistency with KR2020.

² Note that in the SYN1deg dataset the outgoing longwave entropy refers to the entropy of the radiation, so its average is 4/3 of the value $0.928 \text{ mW m}^{-2} \text{ K}^{-1}$ quoted in KR2020. Also, in Eq. (26) of KR2020, $F_{i,\text{LW}}^{\uparrow}$ must be the upward longwave irradiance from the i th level, rather than at it.

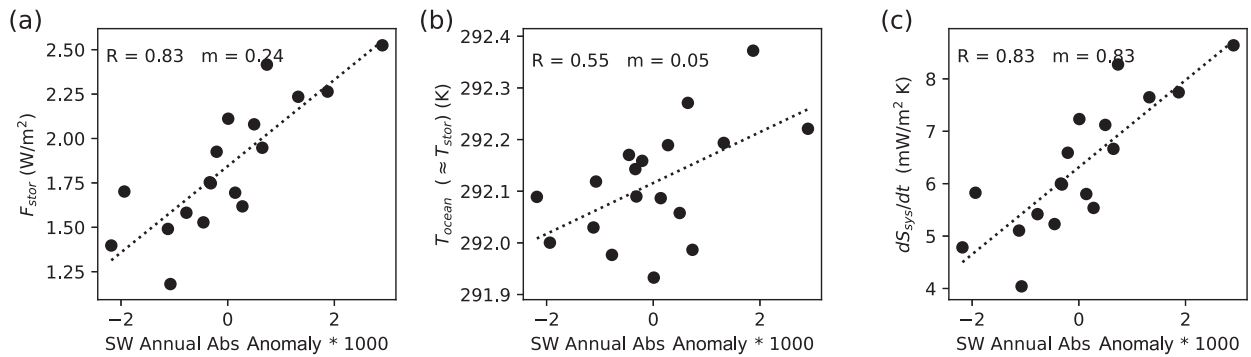


FIG. 1. (a) In the SYN1deg dataset, the rate of storage of energy within the system (the net top-of-atmosphere radiative imbalance) correlates strongly with the top-of-atmosphere solar absorption anomaly. (b) There is also a positive correlation with the average ocean surface temperature (which is used here as a proxy for the entropy storage temperature). (c) The resulting trend in the estimated rate of storage of entropy within the system ($=dS_{\text{sys}}/dt$) has a similar form to the rate of storage of energy, shown in (a). Here, R is correlation coefficient and m is slope.

a. Estimating entropy storage

The entropy content of the climate system is not steady in time but increases as the amount of energy stored in the system increases. The rate of energy storage is the difference in net top-of-atmosphere shortwave incoming irradiance F_{SW} and emitted longwave irradiance F_{LW} : $F_{\text{stor}} = F_{\text{SW}} - F_{\text{LW}}$. It is positively correlated with the solar absorptivity (Fig. 1a): in years with high absorption of solar radiation there is a smaller increase in longwave emission to space because of a damping effect of heat uptake by the ocean (as explored in KR2020's Fig. 8, left and center panels), leading to an increase in energy and entropy storage. More than 90% of this energy is stored in the oceans (Trenberth et al. 2014) and to accurately calculate the entropy change of the ocean due to this heat storage, details of its internal temperature structure would be needed. However, since energy enters and exits the ocean at the surface, the average ocean surface temperature is a reasonable proxy for the internally averaged storage temperature, $T_{\text{stor}} \approx \bar{T}_{\text{ocean}}$. This is lower than the approximation used in Bannon and Najjar (2018), where the energy-influx-weighted ocean temperature is used as the storage temperature; we would argue our approach is appropriate given the role of the cooler deep ocean in heat storage. The ocean temperature also correlates positively with the shortwave absorption anomaly (Fig. 1b), but with much smaller fractional changes than F_{stor} exhibits. These two components can be used to estimate the rate of entropy storage in the climate system, $dS_{\text{system}}/dt \approx F_{\text{stor}}/T_{\text{stor}}$, as shown in Fig. 1c. The variation in the entropy storage rate is dominated by the variation in the energy storage rate, with a mean rate of storage of $6.3 \text{ mW m}^{-2} \text{ K}^{-1}$ in the SYN1deg dataset, with annual means ranging between 4.0 and $8.6 \text{ mW m}^{-2} \text{ K}^{-1}$ in the time period considered.

b. Updated entropy production rate estimates

Figure 2a reproduces the right panel in KR2020's Fig. 8 but uses absolute units rather than anomalies for the difference in longwave outgoing and shortwave absorbed entropy flux (y

axis). This allows us to compare it with the storage rate dS_{system}/dt in Fig. 1c, which shows that the trend in Fig. 2a can be predominately explained by the behavior of storage within the system. In Fig. 2b, the corrected entropy production rate, $\Sigma = J_{\text{out}} - J_{\text{in}} + (dS_{\text{system}}/dt)$, is plotted against the SW annual absorption anomaly. This reveals a trend of entropy production with solar absorption anomaly that is a factor-of-4 smaller in magnitude and of opposite sign, increasing with a slope of 0.13 (95% confidence interval: 0.09 – 0.18) in Fig. 2b rather than decreasing with a slope of -0.70 (95% confidence interval: from -1.06 to -0.47) as in Fig. 2a and in KR2020's Fig. 8 (right panel) for the difference in entropy fluxes.

The mean global entropy production rate over this time period is $81.9 \text{ mW m}^{-2} \text{ K}^{-1}$ (ranging annually between 81.6 and $82.3 \text{ mW m}^{-2} \text{ K}^{-1}$) once annual entropy storage is taken into account, in contrast with the value of $76 \text{ mW m}^{-2} \text{ K}^{-1}$ quoted in KR2020 for the same dataset.

These updated results are not unintuitive. The increase in energy flowing through the system in high absorption years gives more opportunity for entropy production. Higher energy flow drives an increase in the temperature differences within the climate system, which also contributes to the increase in the entropy production rate, $\Sigma_{\text{prod}} = F[(1/T_C) - (1/T_H)]$, where T_H is the representative input temperature and T_C is the output temperature for the irreversible processes. In the time period under consideration, entropy flow is (for an annual average) into, and not out of, the storage, and so T_H is simply the absorption temperature of solar radiation $T_a = F_{\text{SW}}/J_{\text{in}}$. The energy-weighted output temperature is an average of the cooling to space and storage temperatures: $T_C = (F_{\text{LW}} + F_{\text{stor}})/[J_{\text{out}} + (dS/dt)]$. Both temperatures increase with solar absorptivity (Figs. 3a,b), but the effect is small relative to the changes in F_{SW} and F_{LW} , especially when the inverse difference is taken. A common way to express the temperature influence on entropy production is through the Carnot efficiency η , $\eta = 1 - (T_C/T_H) = T_C[(1/T_C) - (1/T_H)]$ (Bannon 2015), such that $\Sigma = \eta F/T_C$. There is a small positive correlation between efficiency and SW absorption anomaly, as shown in Fig. 3c, but the trend in Σ is dominated by the trend in F .

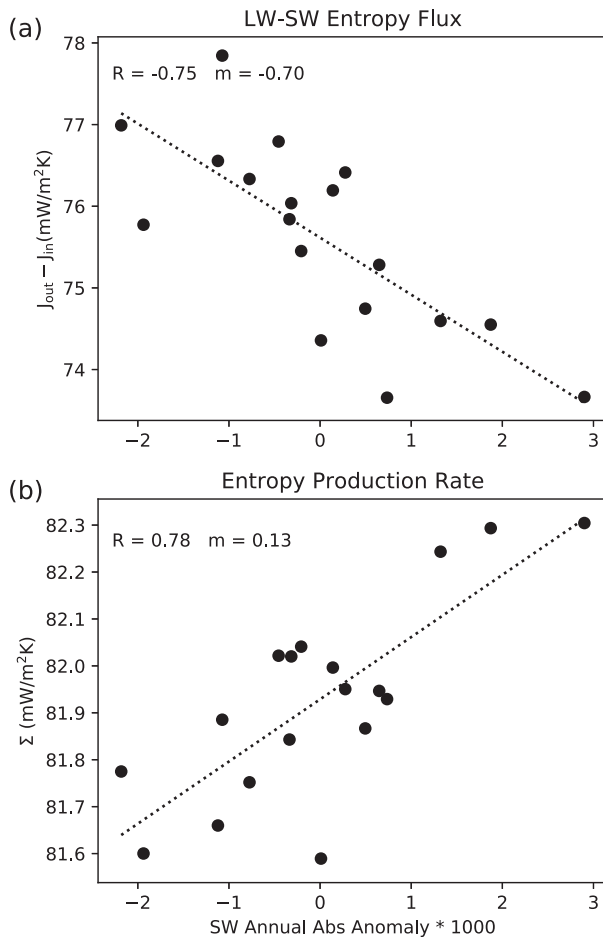


FIG. 2. (a) A reproduction of the right panel of KR2020's Fig. 8 with the y axis, the difference between longwave outgoing entropy and shortwave absorbed, in absolute units rather than anomalies. The downward trend is of a similar order of magnitude to the rate of storage in the system (Fig. 1c). (b) The entropy production rate, calculated by adding the storage to (a), $\Sigma = J_{\text{out}} - J_{\text{in}} + dS_{\text{sys}}/dt$, shows a positive trend. This figure refers to the transfer entropy production rate, as defined in Gibbins and Haigh (2020).

Using the SYN1deg dataset to calculate the F values for consistency, we estimate the storage-corrected average temperature values $T_H = 281.6$ K and $T_C = 256.9$ K and an efficiency of 8.76% (for the transfer perspective), which can be contrasted with the values quoted in Table 3 of KR2020 of $T_a = 282$ K and $T_e = 259$ K where the EBAF dataset is used (incorrectly) to estimate the value of F . The lower value for T_C is striking because it reduces the distance between the observed entropic emission temperature and its theoretical lower limit [see Bannon and Lee (2017), their appendix A], the effective emission temperature $T_e^* = 255$ K.

The storage of entropy in the climate system also impacts the estimate of the nonradiative material entropy production rate and its trend. These trends are of similar form to those for the transfer entropy production rate shown in Fig. 2, with the uncorrected difference in entropy fluxes exhibiting a negative correlation with shortwave absorptivity, with an average value of $49 \text{ mW m}^{-2} \text{ K}^{-1}$,

as in KR2020. With the storage correction, the new estimate for the nonradiative entropy production rate is $55.2 \text{ mW m}^{-2} \text{ K}^{-1}$, the interannual range is $54.9\text{--}55.7 \text{ mW m}^{-2} \text{ K}^{-1}$, and a positive correlation is found between the material entropy production rate and shortwave absorption.

c. Limitations

There are two approximations taken here that limit the accuracy of the numerical results. First, the global average ocean surface temperature is not a precise measure of the average temperature of entropy storage in the climate system, which ought ideally to take account of storage in the deep ocean, the atmosphere, and changes in chemical structure—for example, as glacier mass melts. It would be an interesting but nontrivial project to estimate the annual change in the total entropy content of the Earth system, which could then be used to calculate accurately the representative storage temperature $T_{\text{stor}} = \Delta S_{\text{system}}/\Delta U_{\text{system}}$ from the change in internal energy U . However, because the amount of energy being stored, rather than the temperature of the storage, dominates the trends in Figs. 1 and 2, this would not be expected to influence the qualitative results found. This has been confirmed by testing other estimates for T_{stor} , including an arbitrary constant temperature and the global mean surface temperature, both of which did not dramatically change the results.

Second, inaccuracies in the energy budget in the SYN1deg dataset also limit the applicability of these results. As noted in KR2020, the annual mean rate of energy storage is 1.3 W m^{-2} in the SYN1deg dataset, as compared with 0.71 W m^{-2} in the EBAF dataset, which has been improved by the constraint of observed ocean heating rates (Loeb et al. 2018). However, the estimates of energy and entropy storage from EBAF cannot be combined with entropy flow estimates from SYN1deg because doing so would introduce inconsistencies: a system with less storage ought to have a lower top-of-atmosphere energy imbalance, which in turn would influence the top-of-atmosphere entropy flux imbalance. Using SYN1deg entropy fluxes but energy fluxes from EBAF implies nonconservation of energy.

A more consistent way to combine EBAF energy flux estimates with the entropy flux estimates in the SYN1deg data product is³ to rescale the entropy fluxes by the ratio of energy fluxes in the two datasets: $J_{\text{EBAF}} \approx J_{\text{SYN}}(F_{\text{EBAF}}/F_{\text{SYN}})$. This relies on the assumptions that only the quantity of energy flux and neither the temperature field nor the location of radiative heating differ between data products, which is a reasonable first-order approximation. We find that, with this approach, the estimate for average global transfer entropy production rate is nearly unchanged, at $83 \text{ mW m}^{-2} \text{ K}^{-1}$, with a much lower rate of entropy storage of $2.3 \text{ mW m}^{-2} \text{ K}^{-1}$.

Rederiving the entropy flux as in KR2020 but using a starting dataset with a more accurate top-of-atmosphere energy imbalance would lead to even more accurate entropy budget estimates for the climate.

³ This approach was developed in response to insightful discussions with the KR2020 authors S. Kato and F. G. Rose.

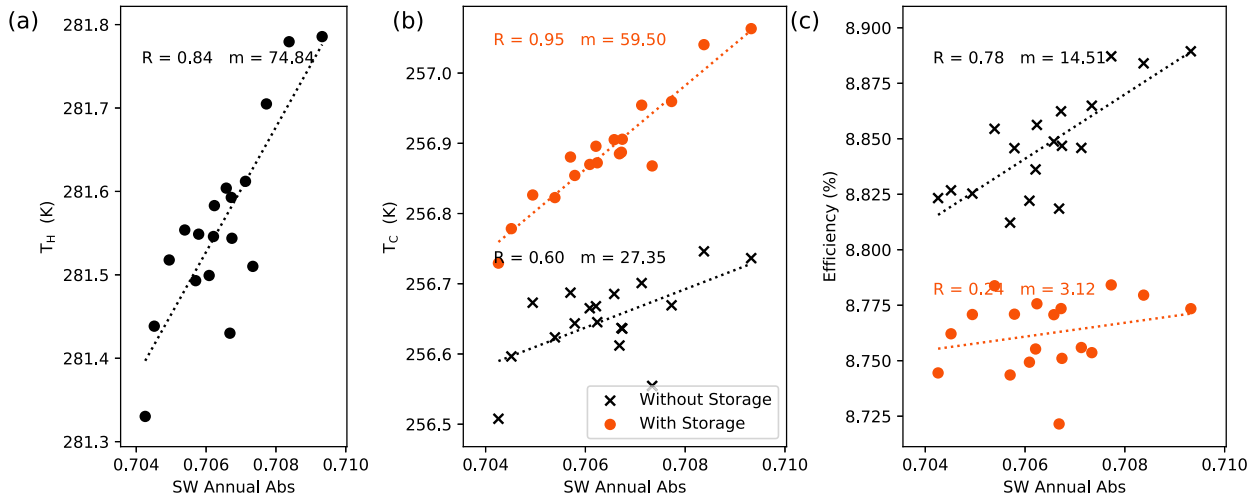


FIG. 3. (a) The energy-averaged shortwave absorption temperature T_H (or T_a in KR2020) increases in high solar absorption years. (b) There is a less pronounced trend in the system's output temperature (black) and in the energy-weighted average of the temperature of radiative emission to space and of storage (red). The values if storage is not accounted for are shown with crosses. (c) The Carnot efficiency of the climate, $1 - (T_c/T_H)$, therefore increases with solar absorptivity. This figure refers to the transfer entropy production view of the climate system (Gibbins and Haigh 2020).

d. Agreement in simple models

The positive correlation of entropy production with shortwave absorption can also be observed in simple climate models. The energy balance model (EBM) described in Bannon (2015) involves two layers: a surface and an atmosphere. Solar radiation is absorbed in the atmosphere (fraction β), and at the surface a portion α is reflected and a portion $(1 - \alpha - \beta)$ is absorbed. Thermal emission of radiation is of the form σT_{surf}^4 for the surface and $\epsilon \sigma T_{\text{atm}}^4$ for the atmosphere. Convective heat flux from the surface to the atmosphere is defined by Bannon (2015) as a fraction of the top-of-atmosphere incoming solar irradiance, but we have reparameterized it here as a function of the surface solar heat flux, $F_{\text{conv}} = \tilde{\gamma} F_{\text{surf,SW}}$, because it is appropriate that it should depend on a more local surface variable. Requiring energy balance for the atmosphere and surface allows those temperatures to be calculated. For the unperturbed model we use parameter values from Bannon (2015): $F_{\text{sun}} = 341 \text{ W m}^{-2}$, $\alpha = 0.30$, $\beta = 0.10$, $\tilde{\gamma} = \gamma/(1 - \alpha - \beta) = 0.42$, and $\epsilon_{\text{atm}} = 0.95$. Details of how material and transfer entropy production rates are calculated in this model can be found in Gibbins and Haigh (2020).

The EBM estimates a steady-state climate configuration; there is no transient response, no seasonality, no interannual variability, and no storage of entropy within the system. However, if the surface albedo α is artificially reduced, the increase in the absorption of solar radiation leads to an increase in the surface and atmospheric temperatures and in the rate of energy flow through the system. Although the absolute value of the entropy production rates in the EBM differ significantly from the observed climate ($\Sigma_{\text{tran}} = 67.0 \text{ mW m}^{-2} \text{ K}^{-1}$ and $\Sigma_{\text{mat}} = 30.4 \text{ mW m}^{-2} \text{ K}^{-1}$), the model produces a strikingly similar fractional increase in the transfer and material entropy

production rates with solar absorptivity when compared with the CERES SYN1deg case (Fig. 4, blue lines).

This is a very different method of leveraging the EBM to estimate an entropy production rate to the approach taken in KR2020. In particular, it is claimed there that “the 1D [two-layer EBM] does not predict the change of T_a with shortwave absorption,” which we would dispute, because in the EBM there is an increase of the average absorption temperature T_a with absorptivity anomaly, $dT_a/da = 107 \text{ K}$, which is comparable to the observed slope of 78 K in Fig. 3a, although the absolute temperatures compare less favorably [$T_{\text{surf}}(\text{EBM}) = 279.3 \text{ K}$ for the observed average albedo of 0.29 as compared with the observed global mean surface temperature in the SYN1deg model of 288 K].

The positive correlation between solar absorption and entropy production rates is also corroborated in the simple analytic radiative–convective model (ARCM) of Robinson and Catling (2012) and Tolento and Robinson (2019) (Fig. 4, red lines). The model approximates the atmosphere as a gray gas in the longwave with two shortwave channels for stratospheric and tropospheric/surface absorption. In the lower portion of the atmosphere, convection is represented by assuming an adjusted adiabatic lapse rate, and temperature and energy flux continuity allows the model to be solved analytically given a small number of physical parameters, including global albedo. Entropy production can be calculated in the ARCM, as explored in Gibbins and Haigh (2020), and gives values for entropy production rates that are again lower than the observed values ($\Sigma_{\text{tran}} = 75.6 \text{ mW m}^{-2} \text{ K}^{-1}$ and $\Sigma_{\text{mat}} = 27.1 \text{ mW m}^{-2} \text{ K}^{-1}$) when using parameter values for Earth given in Tolento and Robinson (2019). When the global top-of-atmosphere albedo is varied, however, the fractional changes in the entropy production rates are broadly consistent with observations (Fig. 4, red lines).

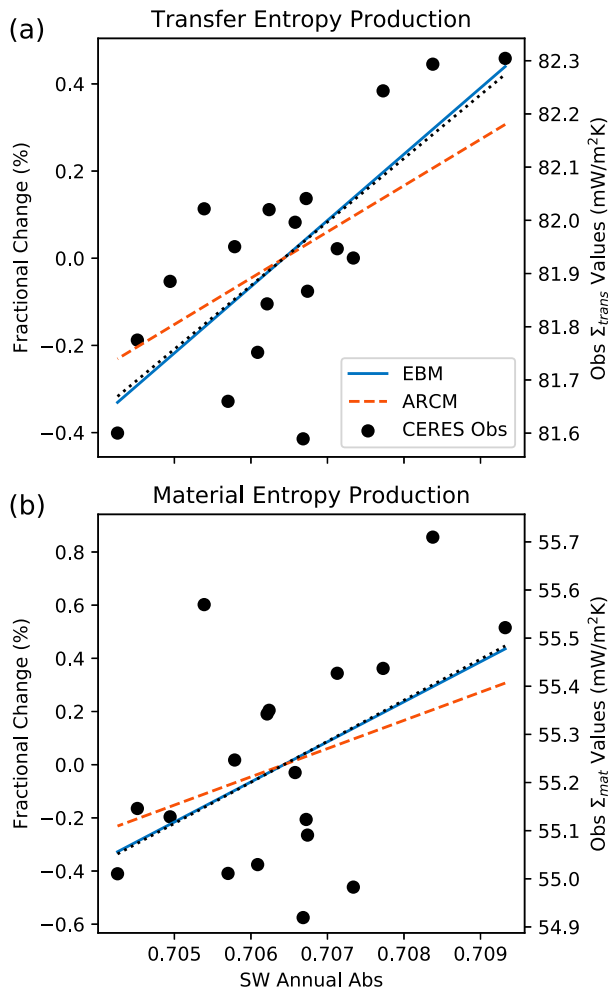


FIG. 4. The fractional change (%) of the entropy production rate with the annual shortwave absorptivity anomaly. The observational CERES SYN1deg data (black filled circles and dotted best-fit line) of Fig. 2 are rescaled by their mean value. The results for entropy production rate changes in response to albedo changes in an energy balance model (blue line) and an analytic radiative-convective model (red line) are compared with their control values [using standard published parameters from Bannan (2015) and Tolento and Robinson 2019]. The slope of the best-fit line in the transfer entropy production case in (a) is 146 units of fractional change (%) per unit absorptivity, with a 95% confidence interval of 70–198, which is consistent with the slopes of the EBM (152) and the ARCM (106). For the material entropy production, the slope of the best-fit line is 154 with a 95% confidence interval from –24 to 266, as compared with the EBM-derived slope of 151 and the ARCM slope of 106.

That the models do not reproduce the absolute values of entropy production rates is not surprising; they contain a very limited range of processes, and in particular they have no horizontal extent, and so any entropy production due to transport in the horizontal is omitted. They are, however, designed to capture the general energy and temperature trends of a climate, especially the increase of energy flux through the system and local temperatures with solar absorption, which are the variables that

determine the entropy production rate. Taken together, the consistency of the positive correlation between top-of-atmosphere shortwave absorption and entropy production in both models *and* observations is strong evidence for that conclusion and underlines the importance of taking entropy storage into account.

The updated results suggest that the transfer entropy production rate increases with solar absorption a as $d\Sigma_{\text{tran}}/da = 120 \text{ mW m}^{-2} \text{ K}^{-1}$ per unit absorptivity (95% confidence interval: 58–161 $\text{mW m}^{-2} \text{ K}^{-1}$). For the material entropy production rate, $d\Sigma_{\text{tran}}/da = 104 \text{ mW m}^{-2} \text{ K}^{-1}$ per unit absorptivity (95% confidence interval: 30–167 $\text{mW m}^{-2} \text{ K}^{-1}$).

4. Conclusions

In our analysis of the entropy flux datasets introduced in KR2020, taking into account the rate of storage of entropy within the climate system uncovers that the global material (nonradiative) and transfer (radiative and nonradiative internal irreversible processes) entropy production rates *increase* with higher solar absorption, in the annual mean and for the CERES SYN1deg satellite-derived record from March 2000 to February 2018. This result is corroborated in an energy balance model and in a simple radiative-convective model but is opposite from the trend identified in KR2020. The significance of this updated result is both in understanding entropy production in the context of the climate and also in indicating how changes in solar absorption influence other aspects of the climate system, which may be relevant for example in discussions of solar radiation management as a climate-restoring approach.

The negative correlation between the net top-of-atmosphere export of entropy with solar absorption highlighted in KR2020 is explained by the increase in storage of entropy within the climate system during high-absorption years, as alluded to in that paper. Incorporating storage also increases estimates of the mean global entropy production rate due to all irreversible (transfer) processes to $81.9 \text{ mW m}^{-2} \text{ K}^{-1}$ and nonradiative (material) processes to $55.2 \text{ mW m}^{-2} \text{ K}^{-1}$, as compared with the values of 76 and $49 \text{ mW m}^{-2} \text{ K}^{-1}$ quoted in KR2020. Improving on our approximation of the temperature of entropy storage in the climate system is a potential avenue for future research. Another is extending the estimates of entropy fluxes to the CERES EBAF dataset in order to more accurately estimate entropy storage rates consistent with the more realistic energy storage rates in that data product.

The influence that the necessary inclusion of storage has on the qualitative as well as quantitative results underlines the importance of rigorous separation between entropy flows, productions, and storage in any analysis of the climate system. Notation and terminology around this point have not yet been settled upon within the community, and it is hoped that the discussion here will progress that conversation.

The global temporally and spatially resolved observational dataset introduced by KR2020 is a very useful resource in global entropy production rate studies, especially given its public availability. We hope that this comment extending their analysis to include the role of entropy storage within the climate system will support its use in further studies.

Acknowledgments. Thanks are given to Seiji Kato and Fred G. Rose whose thoughtful and open conversation enhanced the quality of this exchange. This work was supported by the EPSRC Mathematics of Planet Earth Centre for Doctoral Training, EP/L016613/1.

REFERENCES

- Bannon, P. R., 2015: Entropy production and climate efficiency. *J. Atmos. Sci.*, **72**, 3268–3280, <https://doi.org/10.1175/JAS-D-14-0361.1>.
- , and S. Lee, 2017: Toward quantifying the climate heat engine: Solar absorption and terrestrial emission temperatures and material entropy production. *J. Atmos. Sci.*, **74**, 1721–1734, <https://doi.org/10.1175/JAS-D-16-0240.1>.
- , and R. G. Najjar, 2018: Heat-engine and entropy-production analyses of the World Ocean. *J. Geophys. Res. Oceans*, **123**, 8532–8547, <https://doi.org/10.1029/2018JC014261>.
- Essex, C., 1984: Radiation and the irreversible thermodynamics of climate. *J. Atmos. Sci.*, **41**, 1985–1991, [https://doi.org/10.1175/1520-0469\(1984\)041<1985:RATITO>2.0.CO;2](https://doi.org/10.1175/1520-0469(1984)041<1985:RATITO>2.0.CO;2).
- Gibbins, G., and J. D. Haigh, 2020: Entropy production rates of the climate. *J. Atmos. Sci.*, **77**, 3551–3566, <https://doi.org/10.1175/JAS-D-19-0294.1>.
- Goody, R., 2000: Sources and sinks of climate entropy. *Quart. J. Roy. Meteor. Soc.*, **126**, 1953–1970, <https://doi.org/10.1002/qj.49712656619>.
- , and W. Abdou, 1996: Reversible and irreversible sources of radiation entropy. *Quart. J. Roy. Meteor. Soc.*, **122**, 483–494, <https://doi.org/10.1002/qj.49712253009>.
- Kato, S., and F. G. Rose, 2020: Global and regional entropy production by radiation estimated from satellite observations. *J. Climate*, **33**, 2985–3000, <https://doi.org/10.1175/JCLI-D-19-0596.1>.
- Loeb, N. G., and Coauthors, 2018: Clouds and the Earth's Radiant Energy System (CERES) Energy Balanced and Filled (EBAF) Top-of-Atmosphere (TOA) Edition-4.0 data product. *J. Climate*, **31**, 895–918, <https://doi.org/10.1175/JCLI-D-17-0208.1>.
- Martyushev, L. M., and V. D. Seleznev, 2006: Maximum entropy production principle in physics, chemistry and biology. *Phys. Rep.*, **426**, 1–45, <https://doi.org/10.1016/j.physrep.2005.12.001>.
- Ozawa, H., 2003: The second law of thermodynamics and the global climate system: A review of the maximum entropy production principle. *Rev. Geophys.*, **41**, 1018, <https://doi.org/10.1029/2002RG000113>.
- Paltridge, G. W., 1975: Global dynamics and climate—A system of minimum entropy exchange. *Quart. J. Roy. Meteor. Soc.*, **101**, 475–484, <https://doi.org/10.1002/qj.49710142906>.
- Robinson, T. D., and D. C. Catling, 2012: An analytic radiative–convective model for planetary atmospheres. *Astrophys. J.*, **757**, 104, <https://doi.org/10.1088/0004-637X/757/1/104>.
- Tolento, J. P., and T. D. Robinson, 2019: A simple model for radiative and convective fluxes in planetary atmospheres. *Icarus*, **329**, 34–45, <https://doi.org/10.1016/j.icarus.2019.03.030>.
- Trenberth, K. E., J. T. Fasullo, and M. A. Balmaseda, 2014: Earth's energy imbalance. *J. Climate*, **27**, 3129–3144, <https://doi.org/10.1175/JCLI-D-13-00294.1>.
- Wielicki, B. A., B. R. Barkstrom, E. F. Harrison, R. B. Lee, G. L. Smith, and J. E. Cooper, 1996: Clouds and the Earth's Radiant Energy System (CERES): An Earth observing system experiment. *Bull. Amer. Meteor. Soc.*, **77**, 853–868, [https://doi.org/10.1175/1520-0477\(1996\)077<0853:CATERE>2.0.CO;2](https://doi.org/10.1175/1520-0477(1996)077<0853:CATERE>2.0.CO;2).